

## A Microelectrode Biosensor with Cr/Au Quasi-Triangle Nanodisks for Thyroid-Stimulating Hormone Detection

Di Di<sup>1,\*</sup>, Haoxu Wang<sup>1</sup>, Xuezhong Wu<sup>1</sup>, Peitao Dong<sup>1,2</sup>, Chaoguang Wang<sup>1</sup>, Junfeng Wang<sup>1</sup>, Jian Chen<sup>1</sup>, Shengyi Li<sup>1</sup>

<sup>1</sup>College of Mechatronics and Automation, National University of Defense Technology, Changsha 410073, People's Republic of China

<sup>2</sup>State Key Laboratory of Transducer Technology, Chinese Academy of Sciences, Shanghai 200050, People's Republic of China

\*E-mail: [didi.nudt@gmail.com](mailto:didi.nudt@gmail.com)

Received: 15 February 2014 / Accepted: 23 March 2014 / Published: 14 April 2014

---

Microelectrodes were always used as the sensing components in electrochemical biosensor for the detection of proteins. In this paper, Cr/Au quasi-triangle nanodisks (QTNDs) were fabricated based on colloidal lithography and used to modify a microelectrode biosensor to improve sensitivity. The modified biosensor was composed of two square microelectrodes and Cr/Au QTNDs located in the gap between them. Cr/Au QTNDs can reduce the conductive resistance between electrodes and therefore improve the sensitivity of the biosensors. The fabrication procedure of the sensor was low-cost and high-throughput. Wafer-scale polystyrene (PS) bilayer colloidal crystals (BCCs) were fabricated as templates by spin-coating technology. Some other standard microfabrication methods, such as O<sub>2</sub> reaction ion etching (RIE), metal film deposition and mechanical masking technology, were in turn implemented to fabricate the modified electrochemical sensor. The biosensor was used in the detection of thyroid-stimulating hormone (TSH) based on enzymatic silver deposition reaction. The modified biosensor proved about two times detection sensitivity compared with that without QTNDs. The TSH detection limit can reach 0.005mIU/L. The modified electrochemical biosensors with Cr/Au QTNDs can also be used in the detection of many other kinds of proteins.

---

**Keywords:** Microelectrode biosensor, Thyroid-stimulating hormone, Enzymatic silver deposition reaction, Colloidal lithography, Bilayer colloidal crystal.

### 1. INTRODUCTION

Analysis and detection of low concentrations of biological macromolecules, such as proteins and nucleic acids, is important in the fields of biomedical research and clinical diagnosis [1-4]. Therefore, biosensors with high detection sensitivity have become one of the most important areas of

modern biotechnology. There are many different biosensors such as electrochemical biosensors, thermal biosensors, photochemical biosensors, semiconductor biosensors and acoustic biosensors [2, 4]. Among them, the electrochemical biosensors occupy an important position [1, 3-5]. Especially in recent years, studies of electrochemical biosensors made tremendous progress [1-3, 5-11].

In electrochemical biosensors, the biological recognition signal was usually exchanged to electrical signal (electric current, capacitance or electric voltage), and the biomolecules can be quantitative analyzed [1]. The electrical signal can be led out by solid electrodes, and the structure and size of electrodes have notable influence on sensor precision. Recently, the biosensors using microelectrodes were applied on the high sensitivity detection of some proteins, such as thyroid stimulating hormone (TSH) [12] and prostate specific antigen (PSA) [1]. Sensors based on microelectrodes were advantageous for their compatibility with standard semiconductor technology, and the size of microelectrodes and their gaps determine the detection sensitivity with a great extent [12-16]. However, if the pattern size reduced to below  $1\mu\text{m}$ , the fabrication cost will be sharply increased [13, 16]. Some nanomaterial and structures were therefore introduced to improve the biosensor sensitivity. For example, platinum and silver nanoparticles were used to modify the electrodes for improving the electrochemical sensing capability [11, 17], and nanoparticle probes were used in the electrochemical detection of DNA [16]. However, the fabrication process of the nanostructured biosensor was complex and the introduced nanoparticles were in random distribution on sensor surface.

Colloidal lithography is an attractive tool in the fabrication of high-ordered nanostructures [17-18]. Compared to some standard lithographic nanofabrication techniques (electron beam lithography, focused ion beam lithography (FIB) and scanning probe methods), colloidal lithography provides an inexpensive method with good controllability. Periodic nanostructures based on colloidal lithography, such as nanoholes, nanodots and nanodomes, have been fabricated on the surface of electrodes in some electrochemical biosensors [19-21]. Manufacturing efficiency may be the biggest problem commonly encountered.

In this paper, we demonstrate a simple, fast and low-cost method for the fabrication of a microelectrode biosensor modified by Cr/Au quasi-triangle nanodisks (QTNDs). The electrochemical sensor was composed of two fundamental electrodes and Cr/Au QTNDs located between electrodes, which reduce conducting distance and electric resistance between microelectrodes. The electrochemical biosensors were based on enzyme catalyzed silver deposition and used in the detection of TSH. Experiments proved that the sensor detection sensitivity was improved by inserting metallic nanostructures between electrodes. The fabrication technology was described in the following section. Morphology and electrochemical performance of the sensor were also investigated.

## 2. FABRICATION

The goal of this work is to improve the sensitivity of microelectrode biosensor by introduce metallic nanostructures. For the controllable density and stable electric properties, periodic metallic nanostructures were suitable to be located in the gap of electrodes. In addition, the introduced metallic

nanostructures were hoped to meet the following three conditions: 1, high density distribution; 2, occupy big proportion area of the electrode gap; 3, standing alone on solid substrates. An electrochemical biosensor was selected as prototype, composed of two fundamental electrodes with a 180  $\mu\text{m}$  gap. As shown in fig. 1, the modified electrochemical biosensor was composed of insulated substrates, two square electrodes and Cr/Au QTNDs located in the electrodes gap. The prototype electrochemical biosensor without inserting nanostructures was also fabricated and used to detect TSH as comparison.

The inexpensive and fast fabrication of large area of Cr/Au QTNDs is the key step in this study. Spin-coating technique was employed to fabricate well-organized PS BCCs as shown in fig 2a. PS nanoparticles with average diameter  $347 \pm 15$  nm were used in this paper, and 3-inch (76.2 mm) oxide silicon wafer (oxide layer thickness is 6000Å) was used as substrates. A drop of 1.2 ml PS dispersions (10% w/v in the mixture of water and ethanol v/v=1/1) was spread onto the hydrophilic wafer fixed on spin-coater (EASYLINE-S-200TT, Solar-semi, Germany), and PS BCCs were developed after wafer rotated at 2500 rpm for 1 min. As shown the top view in fig. 2a, the openings formed by two layers of PS beads is small quasi-hexagonal, every edge of which is an arc of PS beads.

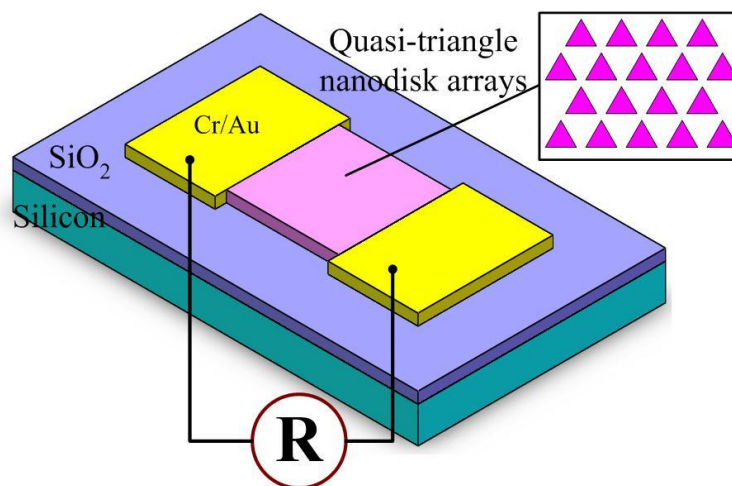


**Figure 1.** Schematic of the microelectrode biosensor modified by Cr/Au QTNDs

$\text{O}_2$  RIE was then used to enlarge the openings between two layers of PS nanoparticles.  $\text{O}_2$  etching was performed in an inductively coupled plasma reactive ion etching system (ICP-2B, from Beijing Chuangweina), operating at  $4.6 \times 10^{-1}$  Pa pressure, 32 SCCM flow rate, 28 W RF power. The total etching time is controlled to be 300s. After  $\text{O}_2$  RIE, the openings shape turned from small quasi-hexagon to quasi-triangle as shown in the top view of fig. 2b. The area of the openings is enlarged many times, which is controllable by etching parameters.

Large area of Cr/Au QTNDs was then fabricated with the sculptured BCCs as mask. Through the quasi-triangle shaped openings shown in fig.2b, Cr/Au was deposited in turn onto wafer surface (fig. 2c). Cr was used here to increase the adhesiveness between Au and substrates. Metal deposition was operated in an e-beam evaporator (ZZS500, from Chengdu Nanguang). The metal deposition rate was about 2~5 Å/s. After PS beads removal, Cr/Au QTNDs were left on the surface of substrates. As

shown in fig. 2d, the fundamental electrodes were fabricated on the metallic nanopatterns by Cr/Au deposition through mechanical mask. At last, the modified electrochemical biosensors with Cr/Au QTNDs were fabricated by the combination of colloidal lithography and MEMS technologies. This fabrication process was simple, stable and fast, without using high precision lithography technologies.

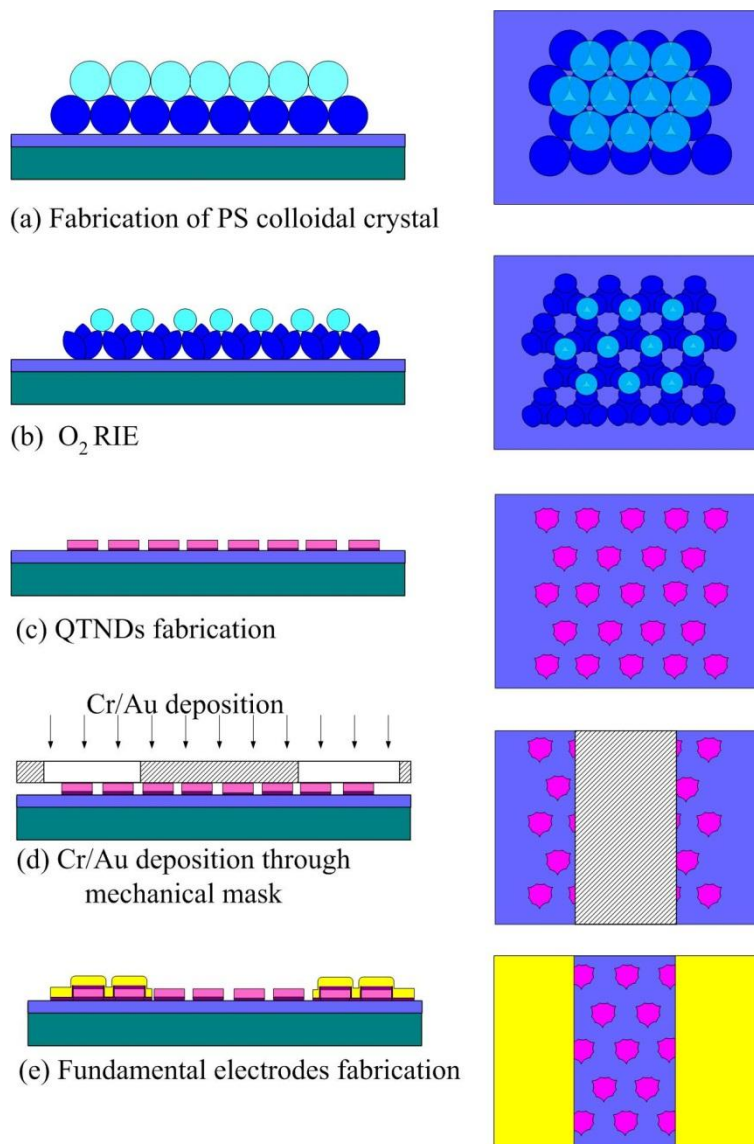


**Figure 2.** Schematic of the fabrication procedure for the modified microelectrode biosensor with Cr/Au QTNDs

### 3. RESULTS AND DISCUSSION

#### 3.1 Morphology analysis

Spin-coating technique is first used to fabricate wafer-scale PS BCCs on insulating substrates, which is inexpensive, fast and good substrate compatibility compared with other self-assembly methods, such as gravity sedimentation technique, vertical deposition method and electrophoretic

deposition methods [22-24]. Fig. 3a shows the photograph of the substrate coated with PS BCCs illuminated on white light. As shown in the photo, the PS BCCs exhibits characteristic six-arm diffraction with  $60^\circ$  angles between adjacent arms, which indicates hexagonal ordering arrangement of PS beads in the long range. Fig. 3b shows the low magnification SEM image of PS BCCs. It can be shown that  $\sim 90\%$  of the substrate was coated with large domains of bilayer colloidal crystal. As in all naturally occurring crystals, some regions include point defects (vacancies), line defects (slip dislocations), and polycrystalline grains. However, these defects have not obvious effect on the density of the templated metallic nanostructures. Fig. 3c-3d shows the top view and side view SEM images of the PS BCCs. As shown in Fig. 3c, the upper layer and lower layer are both hexagonal-close-packed PS beads.

To enlarge the openings between two layers of PS beads, PS BCCs was then sculptured by  $O_2$  RIE. Fig. 4a~b shows the high and low magnification SEM images of PS BCCs after 300s RIE. As shown in fig.4b, the upper PS beads have been reduced to much smaller nanoparticles, and the particle surface was rather rough. In etching process, the shadowed part of lower beads becomes gradually smaller with the upper beads, and the lower beads were finally sculptured to three-petals-like shape as mentioned in [17]. The bilayer nanostructures remained hexagonal ordered arrangement after  $O_2$  RIE. As shown in fig. 4, the openings shape turns from small quasi-hexagon to big quasi-triangle. The area and shape of the openings can be adjusted by controlling the RIE parameters. Although the openings were enlarged many times, they were still not easy to be connected with each other until the upper beads disappeared.

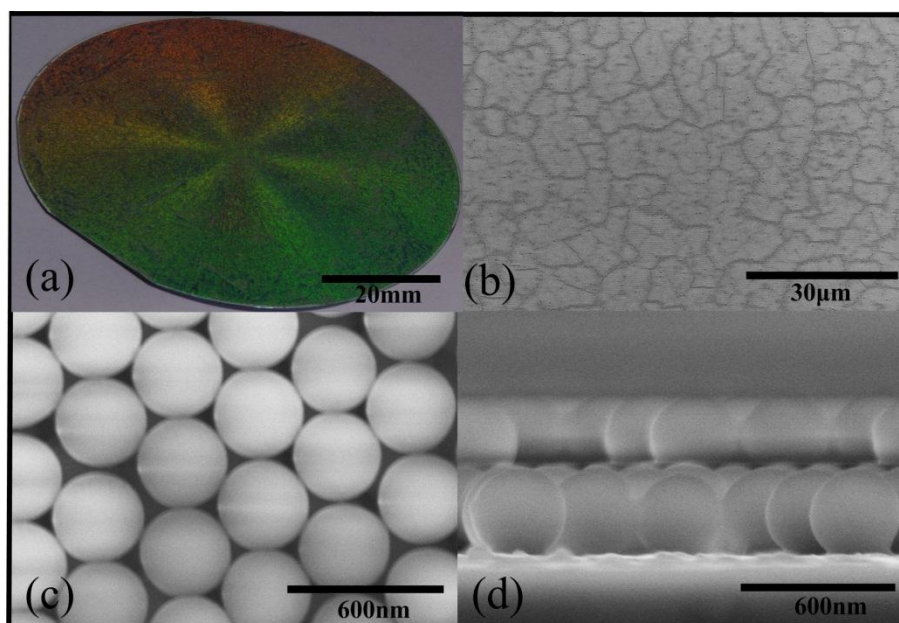


**Figure 3.** (a) the white light reflection photo of wafer-scale PS BCCs; (b~c) respectively low magnification and high magnification of top view SEM images of PS BCCs; (d) the side view SEM image of the PS BCCs.

With etched PS BCCs as mask, Cr/Au QTNDs were developed by metal deposition through the quasi-triangle openings. After PS beads removal, wafer-scale Cr/Au QTNDs were left on substrates.

The fundamental electrodes were then fabricated by metal deposition onto nanopatterns through mechanical mask, and used as the output port of electrical signal in the following measurements.

Fig.4c~d shows the low and high magnification SEM images of Cr/Au QTNDs located in the gap between two fundamental electrodes. As shown in fig. 4c, the templated QTNDs kept the shape, size and the array arrangement well with the openings formed by the etched PS BCCs as shown in fig. 4a. The shape of Cr/Au nanodisk is quasi-triangle, and the length of three sides is theoretically equal because of their structural symmetry. Learning from the pixel calculation of fig. 4c by measurement software, Cr/Au QTNDs occupied about 40% area between the fundamental electrodes. Nanodots can also be fabricated based on monolayer colloidal crystal, and the theoretically occupied area is about 9.3% when no particles adhesive with each other. In reality, there is usually serious adhesion between self-assembled colloidal particles. Nanodots based on monolayer colloidal crystal were used to increase the electrode surface area in electrochemical sensor [20]. The metallic QTNDs developed in this paper occupied much bigger area.

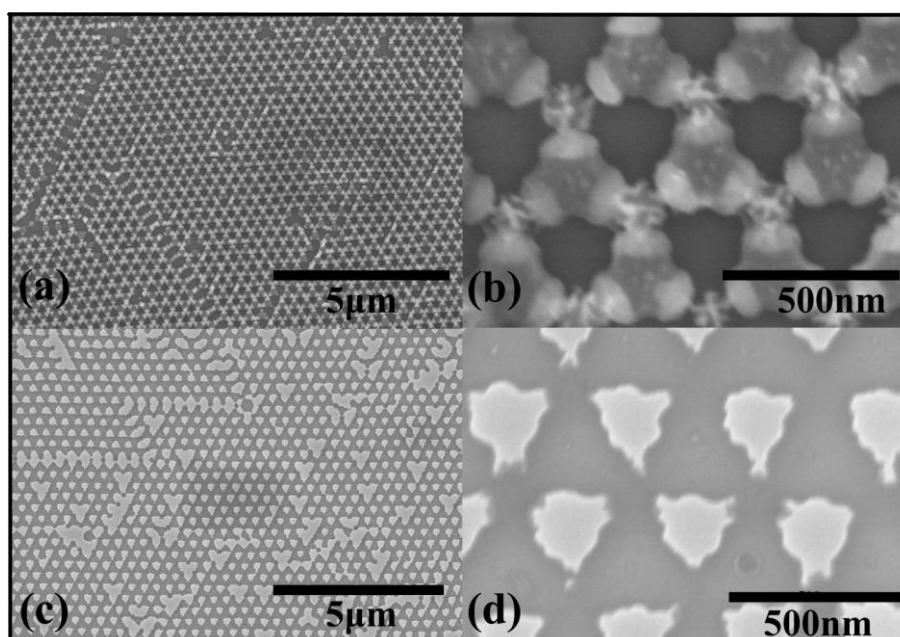


**Figure 4.** (a-b) The low and high magnification SEM images of PS BCCs after 300s O<sub>2</sub> RIE; (c-d) The low and high magnification SEM images of the template Cr/Au QTNDs.

### 3.2 Electrochemical performance of the modified biosensors

Application of colloidal lithography based nanopatterns lead to a variety of applications and favorable characteristics towards electrochemical sensing devices [19-21]. The microelectrode biosensor modified by Cr/Au QTNDs employs the enzyme-linked immunosorbant assays technique to capture TSHs and makes use of enzymatic silver deposition reaction to detect TSHs. The preparation process and the detection strategy of the biosensor were illustrated in Fig. 5. First, the biosensor was immersed in ethanol solution containing 2.5% APTES ((3-aminopropyl) triethoxysilane) and 1% H<sub>2</sub>O for 24h, in order to immobilize APTES molecules on the surface of the wafer. Then the biosensor was

immersed in 5.0% glutaraldehyde solution for 1h (fig. 5a), to connect the glutaraldehyde on the APTES molecules. Second, the substrate was incubated in PBS solution (0.01 mol/L phosphate buffer saline in 0.1 mol/L NaCl, pH 7.4) containing capture monoclonal antibody (mAb) at 37°C for 1 h, then the capture mAb was modified on the biosensors. Then, the substrate was incubated in 1% bovine serum albumin (BSA) at 37°C for 1h to block non-specific adsorption sites on the substrate as shown in Fig. 5b. Then the modified biosensor could be used to test the TSH.

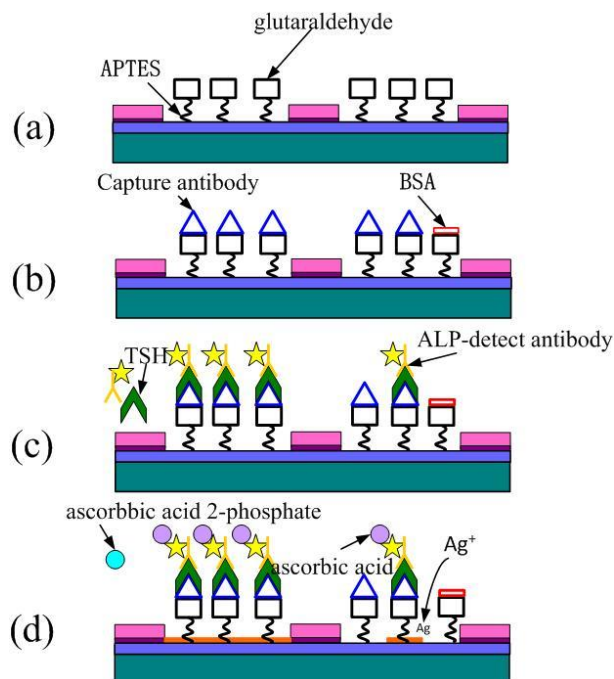


**Figure 5.** Schematic representation of the preparation process and the detection strategy for TSH with the modified biosensor

After the capture mAb was immobilized in the gaps as a catcher, the TSH antigen and Alkaline phosphatase (ALP)-detect mAb was added on the biosensor, and then incubated at 37°C for 30 min. As shown in fig. 5c, a capture mAb/TSH/ALP-detect mAb sandwich structure was developed among the gaps of Cr/Au QTNDs. Next, the silver deposition solution (0.1mol/L glycine-NaOH containing 1mmol/L ascorbic acid 2-phosphatase (AAP) and 5 mmol/L  $AgNO_3$ , pH 9.0) was added on the biosensor and incubated at 37 °C for 10 min in the dark. AAP was catalyzed by ALP connected with detect antibody to be ascorbic acid, and  $Ag^+$  was reduced to Ag deposit on the biosensor surface as show in fig. 5d.

Finally, an electrochemical workstation (Autolab) was used to measure the electrochemical performance of this biosensor in the room temperature. The linear sweep voltammetry curve was collected within a potential range from 0 to 50mV. The electrical conductance between two electrodes can be calculated quantitatively from the recorded curve of current against potential. The goal of this work is to prove the sensitivity improvement of the TSH biosensor modified by Cr/Au QTNDs. The modified and prototype biosensor were both used to detect TSH of 1mIU/L concentration.

Fig. 6 shows the linear sweep voltammetry curves after measurements. The blue curve is the measured curve of the modified biosensor with Cr/Au QTNDs, black curve is the prototype biosensor. The red curve is the comparison sample without enzymatic silver deposition reaction. It can be shown that the modified biosensor can provide two times sensitivity of that without QTNDs, so it can detect TSH as low as 0.005mIU/L. In the modified biosensor, the distance between two electrodes is constant, but the conductive nanostructure arrays in the gap can reduce the conducting distance. When the TSH of same concentration is tested, the modified biosensor has a lower resistance of the Ag precipitate, and provides a higher conductance, so the low-level hormones can be detected by the modified biosensor.

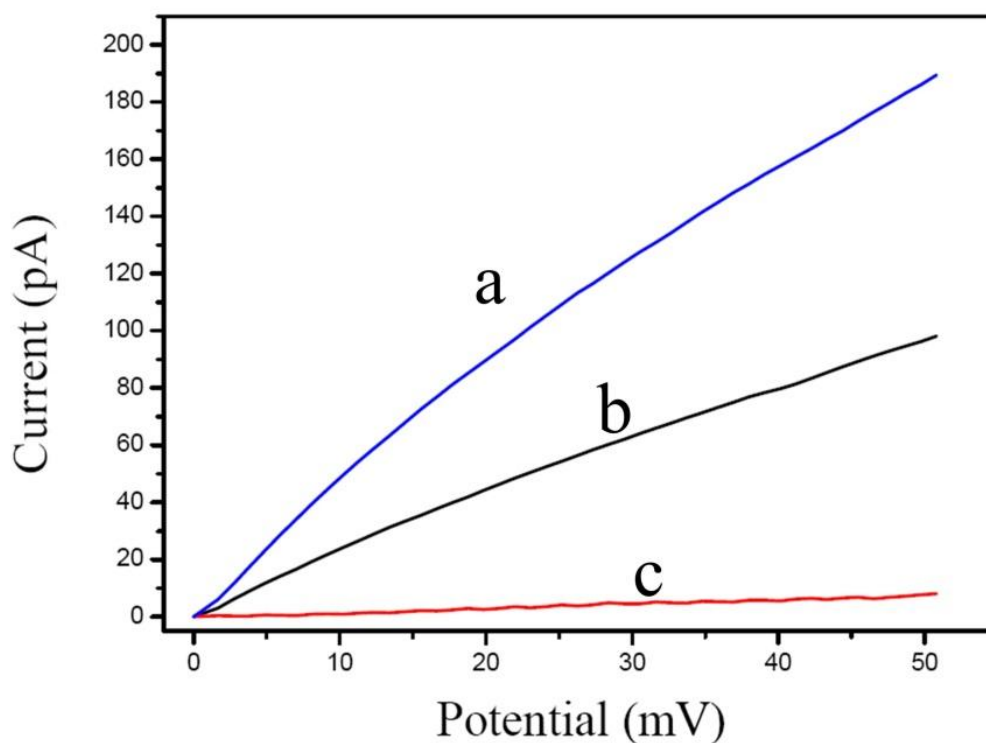


**Figure 6.** Linear sweep voltammetry curves of (a) modified biosensor with Cr/Au QTNDs; (b) prototype biosensor without Cr/Au QTNDs; (c) comparison sample without enzymatic silver deposition reaction.

The measuring results indicated that, metallic nanostructures based on colloidal lithography technologies can be used to improve the sensitivity of electrochemical biosensor. It will be studied in the future for the fabrication of nanostructures with smaller gaps and larger occupied area.

#### 4. CONCLUSION

In this paper, a low-cost and high-throughput method based on colloidal lithography is developed for fabricating Cr/Au QTNDs and putting them at the desired location in microelectrode biosensors, with controllable shape, period and size. The modified microelectrode biosensor was

composed of two fundamental microelectrodes and Cr/Au QTNDs located in the microgap between them. Wafer-scale PS BCCs was first fabricated as templates by spin-coating technology. Large area of Cr/Au QTNDs was developed on substrates following by O<sub>2</sub> RIE, metal deposition and lifting-off process. The fundamental electrodes were fabricated onto the metallic nanopatterns by metal deposition through mechanical mask. Cr/Au QTNDs were located in the gap of fundamental electrodes, which can reduce the conductive distance between electrodes and improve the sensitivity. The improved biosensor is used to detect TSH and has proved to have about two times detection sensitivity. Cr/Au QTNDs can also be introduced in other electrochemical biosensor with microelectrodes for sensitivity improvement.

#### ACKNOWLEDGEMENTS

The authors would like to thank the financial support provided by National Natural Science Foundation of China (91023028), the Foundation of State Key Laboratory of Transducer Technology (SKT1201) and the Doctoral Interdisciplinary Joint Training of NUDT (kxk130302).

#### References

1. Y. Huang, T.H. Wang, J.H. Jiang, G. L. Shen and R. Q. Yu, *Clin. Chem.*, 51(2009) 964.
2. D. Grieshaber, R. MacKenzie, J. Vörös and E. Reimhult, *Sensors*, 8(2008) 1400.
3. M.D. Vestergaard, K. Kerman and E. Tamiya, *Sensors*, 7(2007) 3442.
4. J. Wang, *Microchim. Acta.*, 177(2012) 245.
5. K. Kerman, M. Chikae, S. Yamamura, E. Tamiya, *Anal. Chim. Acta.*, 588(2007) 26.
6. Y.F. Xu, M. Velasco-Garcia, T.T. Mottram, *Biosens. Bioelectron.*, 20(2005) 2061.
7. S. Cagnin, M. Caraballo, C. Guiducci, P. Martini, M. Ross, M. SantaAna, D. Danley, T. West and G. Lanfranchi, *Sensors*, 9(2009) 3122.
8. A.S. Rad, M. Jahanshahi, M. Ardjmand, A.A. Safekordi, *Int. J. Electrochem. Sci.*, 7(2012) 2623.
9. R.M. Iost, J.M. Madurro, A.G. Brito-Madurro, I.L. Nantes, L. Caseli, F.N. Crespilho, *Int. J. Electrochem. Sci.*, 6 (2011) 2965.
10. U. Yogeswaran and S.M. Chen, *Sensors*,8(2008) 290.
11. A.S. Rad, A. Mirabi, E. Binaian and H. Tayebi, *Int. J. Electrochem. Sci.*,6(2011) 3671.
12. H.X. Wang, X.Z. Wu, P.T. Dong, C.G. Wang, J.F. Wang, Y.Z. Liu and J. Chen, *Int. J. Electrochem. Sci.*, 9(2014) 12.
13. J.S. Shim, M.J. Rust and C.H. Ahn, *J. Micromech. Microeng.*, 23(2013) 035002.
14. H.X. Wang, P.T. Dong, D. Di, C.G. Wang, Y.Z. Liu, J.F. Wang, J. Chen and X.Z. Wu, *Micro Nano Lett.*, 8 (2013) 11.
15. Q. Humayun, M. Kashif and U. Hashim, *J. Nanomater.*, 2013(2013) 301674.
16. Y.T. Cheng, C.C. Pun, C.Y. Tsai and P.H. Chen, *Sens. Actuators-B.*, 109(2005) 249.
17. C. Qian, C. Ni, W.X. Yu, W.G. Wu, H.Y. Mao, Y.F. Wang and J. Xu, *Small*, 7(2011) 1801.
18. P. Colson, C. Henrist and R. Cloots, *J. Nanomater.*, 2013(2013) 948510.
19. T. Lohmüller, U. Müller, S. Breisch, W. Nisch, R. Rudolf, W. Schuhmann, S. Neugebauer, M. Kaczor, S. Linke, S. Lechner, J. Spatz and M. Stelzle, *J. Micromech. Microeng.*, 18(2008) 115011.
20. A. Tsigara, A. Benkhial, S. Warren, F. Akkari, J. Wright, F. Frehill and E. Dempsey, *Thin solid Films*, 537(2013) 269.
21. A. Lupu, A. Valsesia, F. Bretagnol, P. Colpo and F. Rossi, *Sens. Actuators-B.*, 127(2007) 606.
22. Z.Q. Sun and B. Yang, *Nanoscale. Res. Lett.*, 1(2006)46.
23. A. L.Rogach, N.A. Kotov, D. S. Koktysh, J. W. Ostrander and G. A. Ragoisha, *Chem. Mater.*

12(2000)2721.

24. S. M. Yang, S. G. Jang, D. G. Choi, S. Kim and H. K. Yu, *Small*, 4(2006)458.

© 2014 The Authors. Published by ESG ([www.electrochemsci.org](http://www.electrochemsci.org)). This article is an open access article distributed under the terms and conditions of the Creative Commons Attribution license (<http://creativecommons.org/licenses/by/4.0/>).